www.nature.com/npp

American College of Neuropsychopharmacology

ARTICLE

Kappa opioid receptor modulation of excitatory drive onto nucleus accumbens fast-spiking interneurons

Benjamin C. Coleman[1], Kevin M. Manz[2,3,4] and Brad A. Grueter[1,4,5,6,7]✉

The dynorphin/kappa opioid receptor (KOR) system within the nucleus accumbens (NAc) contributes to affective states. Parvalbumin fast-spiking interneurons (PV-FSIs), a key component of feedforward inhibition, participate in integration of excitatory inputs to the NAc by robustly inhibiting select populations of medium spiny output neurons, therefore greatly influencing NAc dependent behavior. How the dynorphin/KOR system regulates feedforward inhibition in the NAc remains unknown. Here, we elucidate the molecular mechanisms of KOR inhibition of excitatory transmission onto NAc PV-FSIs using a combination of whole-cell patch-clamp electrophysiology, optogenetics, pharmacology, and a parvalbumin reporter mouse. We find that postsynaptic KOR stimulation induces long-term depression (LTD) of excitatory synapses onto PV-FSI by stimulating the endocytosis of AMPARs via a PKA and calcineurin-dependent mechanism. Furthermore, KOR regulation of PV-FSI synapses are input specific, inhibiting thalamic but not cortical inputs. Finally, following acute stress, a protocol known to elevate dynorphin/KOR signaling in the NAc, KOR agonists no longer inhibit excitatory transmission onto PV-FSI. In conclusion, we delineate pathway-specific mechanisms mediating KOR control of feedforward inhibitory circuits in the NAc and provide evidence for the recruitment of this system in response to stress.

Neuropsychopharmacology (2021) 46:2340–2349; https://doi.org/10.1038/s41386-021-01146-8

INTRODUCTION

The nucleus accumbens (NAc) is a key node within the mesolimbic dopamine system, integrating glutamatergic input from limbic, cortical, and thalamic brain regions to drive motivated behavior [1, 2]. Experience dependent plasticity of these inputs has been shown to underlie maladaptive motivational states [2–7]. NAc-dependent motivational output is organized by networks of parvalbumin-expressing fast-spiking interneurons (PV-FSIs) that gate medium spiny neuron (MSN) output via feedforward inhibition [8–13]. For example, inhibition of NAc PV-FSIs increases impulsivity and decreases psychostimulant induced associative learning [14, 15]. Studies from our lab and others indicate that feedforward glutamatergic synapses onto PV-FSIs exhibit multiple molecularly distinct modes of plasticity, each proceeding via G-protein-coupled receptor (GPCR)-dependent mechanisms [10, 11, 16, 17]. However, it is unknown whether endogenous opioid signaling, a neuromodulatory system critically involved in adaptive and pathological reward behavior, modulates PV-FSI-embedded feedforward microcircuits.

The dynorphin/kappa opioid receptor (KOR) system is heavily implicated in stress, stress induced reinstatement of drug seeking, as well as negative affective states during withdrawal [18–21]. Importantly, recruitment of the dynorphin/KOR system in the NAc is aversive [22–24], and dynorphin is increased in the NAc of individuals with cocaine use disorder and suicidal ideologies, as well as in rodent models of addiction and depression [25–28]. KORs are Gαi-coupled GPCRs that dynamically and heterosynaptically regulate glutamate release in the NAc, highlighting the importance of KORs as key mediators of NAc signal transduction [29–33]. How KORs modulate PV-FSI-embedded feedforward microcircuits, and PV-FSI relevant behaviors, represent an important gap in understanding how this receptor influences NAc circuit activity. We examined prefrontal cortex (PFC) and midline nuclei of the thalamus (mThal) inputs into the NAc as they regulate opposing behaviors. Stimulation of PFC—NAc afferents promotes real-time place preference, and stimulation of mThal—NAc afferents promotes real-time place aversion [5, 34].

We used whole-cell patch-clamp electrophysiology, transgenic mice, and behavioral manipulations paired with pharmacology to probe the dynorphin/KOR system at excitatory inputs onto NAc core (NAcc) PV-FSIs. We report that postsynaptic KORs diminish feedforward drive onto NAcc PV-FSIs via AMPAR endocytosis through a PKA/calcineurin-dependent mechanism. Interestingly, we also find that mThal afferents onto PV-FSIs are preferentially regulated by KORs over PFC afferents. To test for in vivo recruitment of the KOR system we used immobilization stress. Acute immobilization stress prevented KOR-induced depression of excitatory transmission onto NAcc PV-FSIs. Importantly, KOR-dependent long-term depression (LTD) was recovered by pre-exposure to the KOR antagonist nor-BNI, suggesting the

[1]Department of Pharmacology, Vanderbilt University, Nashville, TN, USA. [2]Medical Scientist Training Program, Vanderbilt University, Nashville, TN, USA. [3]Neuroscience Graduate Program, Vanderbilt University, Nashville, TN, USA. [4]Vanderbilt Brain Institute, Vanderbilt University, Nashville, TN, USA. [5]Department of Anesthesiology, Vanderbilt University Medical Center, Nashville, TN, USA. [6]Vanderbilt Center for Addiction Research, Vanderbilt University, Nashville, TN, USA. [7]Department of Molecular Physiology and Biophysics, Vanderbilt University, Nashville, TN, USA. ✉email: brad.grueter@vumc.org

Received: 19 April 2021 Revised: 30 June 2021 Accepted: 3 August 2021
Published online: 16 August 2021

involvement of this mechanism in response to acute stress. Together, these findings provide novel insight into mechanisms by which the endogenous dynorphin/KOR system regulates feedforward drive in the NAcc and implicates KORs on NAcc PV-FSIs in acute stress.

MATERIALS AND METHODS

Animals

Mice were housed in the Vanderbilt University Medical Center animal care facility in accordance with Institutional Animal Care and Use Committee guidelines. Mice were group housed 2–5/cage with *ad lib* access to food and water and kept on a 12-h light-dark cycle. Male and female mice ages 7–12 weeks were used for all experiments. No differences were found between sexes, so data was combined. To allow for fluorescent visualization of PV-FSIs in electrophysiology experiments, Cre-induced $STOP^{fl/fl}$-tdTomato mice (Ai9, $Gt(ROSA)26Sor^{tm9(CAG\text{-}tdTomato)Hze}$) (Jackson Laboratory Stock No.: 007909) were crossed with parvalbumin (PV) PV-IRES-Cre mice (PV^{Cre}, $Pvalb^{tm1(cre)Arbr/J}$, Stock No.: 008069), generating PV^{Cre}-$tdTomato^{fl/fl}$ (PV^{tdT}) mice.

Electrophysiology

For detailed electrophysiological methods see [35]. In brief, PV^{tdT} mice were killed under isoflurane anesthesia, brain dissected, and sagittal brain slices 250 µm thick prepared using a Leica VT1200S Vibratome. Slices were prepared in oxygenated (95% O2; 5%CO2) ice-cold *N*-methyl-*D*-glucamine (NMDG)-based solution (in mM: 2.5 KCl, 20 HEPES, 1.2 NaH_2PO_4, 25 Glucose, 93 NMDG, 30 $NaHCO_3$, 5.0 sodium ascorbate, 3.0 sodium pyruvate, 10 $MgCl_2$, and 0.5 $CaCl_2$-$2H_2O$) and recovered for 10 min in the same solution at 34 °C. Slices were then recovered for 1 h in oxygenated artificial cerebrospinal fluid (ACSF) containing (in mM: 119 NaCl, 2.5 KCl, 1.3 $MgCl_2$-$6H_2O$, 2.5 CaCl2-$2H_2O$, 1.0 NaH_2PO_4-H_2O, 26.2 $NaHCO_3$, and 11 glucose; 287–295 mOsm). During experiments, slices were continuously perfused with oxygenated ACSF containing 50 µM picrotoxin ($GABA_AR$ antagonist to isolate excitatory postsynaptic currents; EPSCs) at a rate of 2 mL/min and a temperature of 32 ± 2 °C. To isolate miniature (m) EPSCs, tetrodotoxin (1 µM) was added to the ACSF. PV^{tdT} cells in the NAcc were visualized using Scientifica PatchVision software via 530 nm LED light. PV-FSIs were confirmed according to biophysical properties (capacitance, membrane resistance, and AMPAR decay kinetics) [11, 17].

Whole-cell patch-clamp electrophysiology was performed using a CV-7B headstage, Multiclamp 700B Amplifier, Axopatch Digidata 1550 digitizer, and 3-6 MΩ glass recording micropipettes (Sutter P1000 Micropipette Puller). Voltage clamp recordings were done at −70 mV using a K^+-based intracellular solution (in mM: 135 K^+-gluconate, 5 NaCl, 2 MgCl2, 10 HEPES, 0.6 EGTA, 3 Na2ATP, 0.4 Na2GTP; 285-292 mOsm). For experiments using GDPβS trilithium salt, Na2GTP was excluded from the internal solution and 1 mM GDPβS added. BAPTA (10 mM), D15 (2 mM), S15 (2 mM) were added to the internal solution as indicated. In these subsets of experiments, cells were dialyzed for 30 min prior to the beginning of the recording.

A bipolar electrode was placed at the cortico-accumbens interface and stimulated at 0.1 Hz to examine local neurotransmission. Paired-pulse ratio (PPR) was acquired within experiment by giving two 0.15 ms pulses with a 50 ms interstimulus interval and dividing the amplitude of the second EPSC by the first. For experiments examining mThal or PFC synapses onto NAcc PV-FSIs, 473-nm Cool LED stimulation was delivered at 0.1 Hz with a 0.3-ms pulse duration to slices prepared from mice expressing ChR2 on terminals within the NAcc. Cells with a >15% change in series resistance (Rs) we excluded from analysis.

Immobilization stress

For immobilization stress experiments, mice were constrained in a cylindrical tube for 1 h, allowed to recover for 10 min, and then sacrificed for electrophysiology. KOR antagonist, nor-BNI (10 mg/kg), or saline was administered by intraperitoneal (IP) injection 24 h prior to immobilization stress.

Stereotaxic injections

To probe input specificity, mice underwent stereotaxic surgery for viral-mediated gene transfer of channel rhodopsin (ChR2). At ~4 weeks of age mice were given bilateral injections (400nL) of AAV5-CaMKII-ChR2-EYFP (Addgene, Watertown, MA) and killed 3-5 weeks after surgery for electrophysiological experiments. Coordinates were (relative to bregma): mThal (medial-lateral (ML): ±0.3, anterior-posterior (AP): −1.2, dorsal-ventral (DV): −3.0) or PFC (ML: ±0.3, AP: −1.75, DV: −2.75).

Pharmacology

1-Naphthyl acetyl spermine (NASPM) trihydrochloride, isoflurane, tetrodotoxin, (-)-U50488 hydrochloride, and nor-binaltorphimine dihydrochloride, were obtained from Tocris/Bio-Techne, Minneapolis, MN. Picrotoxin, BaCl2, and GDPβS trilithium salt were obtained from Sigma-Aldrich, St. Louis, MO. D15 (PPPQVPSRPNRAPPG) and S15 (ANVRRGPPPPPQPSP) were synthesized by Bio-Synthesis Inc. Lewisville, TX.

Statistics

Clampfit 10.4 and GraphPad Prism v7.0 were used to analyze all experiments. Changes in EPSC amplitude, EPSC frequency, coefficient of variance (CV), and PPR were calculated by comparing the mean values during the first 5 or 10 min (defined for each experiment) to the mean values in during the final 5 or 10 min of each experiment. Each data point represents the average of one cell, n = number of cells N = number of mice. Paired or unpaired t tests were used. Errors bars represent SEM. For all analyses, $p < 0.05$ was considered significant.

RESULTS

The dynorphin/KOR system triggers LTD of excitatory drive onto NAcc PV-FSIs

KORs depress excitatory synapses onto NAc MSNs by inhibiting glutamate release, however, their function at PV-FSIs is unknown [31, 36, 37]. To determine the contribution of KORs to excitatory drive onto NAcc PV-FSIs, we tested KOR pharmacology on electrically evoked EPSCs (eEPSC). Application of the endogenous KOR agonist, dynorphin A, elicited a depression of eEPSCs (Fig. 1B, D, F; Dyn. A: 75.0 ± 5.8%, $n = 7$, $p = 0.005$, paired t test). To gain KOR specificity, as dynorphin A exhibits activity at the mu and delta opioid receptors, we used KOR selective agonist (-)-U-50488. Consistent with dynorphin A, U-50488 triggered a decrease in eEPSC amplitude that persisted in the presence of KOR antagonist, nor-binaltorphimine (nor-BNI), indicating LTD (Fig. 1C, E, F U-50488: 71.4 ± 5.4%, $n = 7$, $p = 0.002$, paired t-test). To further ensure the specificity of the observed effect to KORs, we washed on the agonist U-50488 in the presence of nor-BNI and observed no depression (Fig. 1G; U-50488 in nor-BNI: 95.7 ± 4.0%, $n = 8$, $p = 0.31$, paired t test). Furthermore, KORs lack tonic regulation of excitatory drive onto PV-FSIs exemplified by no change in the eEPSC amplitude following the application of nor-BNI (Fig. 1H 105.5 ± 5.2%, $n = 8$, $p = 0.327$, paired t test). These data demonstrate LTD of excitatory drive onto NAcc PV-FSIs by KORs.

KOR triggered LTD is expressed post-synaptically

To determine whether KOR-induced LTD is expressed pre- or post-synaptically, we examined PPR and coefficient of variance (CV), metrics which are inversely correlated with release probability. Consistent with a postsynaptic locus of action, we observed no significant changes in either PPR (50 ms) or CV (Fig. 2A; PPR baseline: 1.32 ± 0.05; PPR 40–50 min: 1.38 ± 0.05, $n = 7$, $p = 0.25$, paired t test) (Fig. 2B; CV baseline: 0.18 ± 0.02; CV 40–50 min: 0.18 ± 0.02, $n = 7$, $p = 0.84$, paired t test). However, presynaptic KOR mediated depression of EPSCs have been reported with no observable change in PPR [33]. Therefore, we incorporated TTX-insensitive mEPSC analyses in response to pharmacological activation of KORs. mEPSCs were analyzed during the first 5 min and from minutes 40–45 of U-50488 application experiments. U-50488 elicited no change in mEPSC frequency while significantly decreasing amplitude, consistent with a decrease in post-synaptic response to neurotransmitter release (Fig. 2C; frequency 0–5 min: 10.26 ± 1.53 Hz; frequency 40–45 min: 10.40 ± 1.61 Hz, $n = 10$, $p = 0.87$, paired t test; amplitude 0-5 min: 18.78 ± 0.91 pA; amplitude 40–45 min: 16.75 ± 0.72 pA, $n = 10$, p = 0.042, paired t-test). To further validate the postsynaptic action of KOR-mediated LTD of

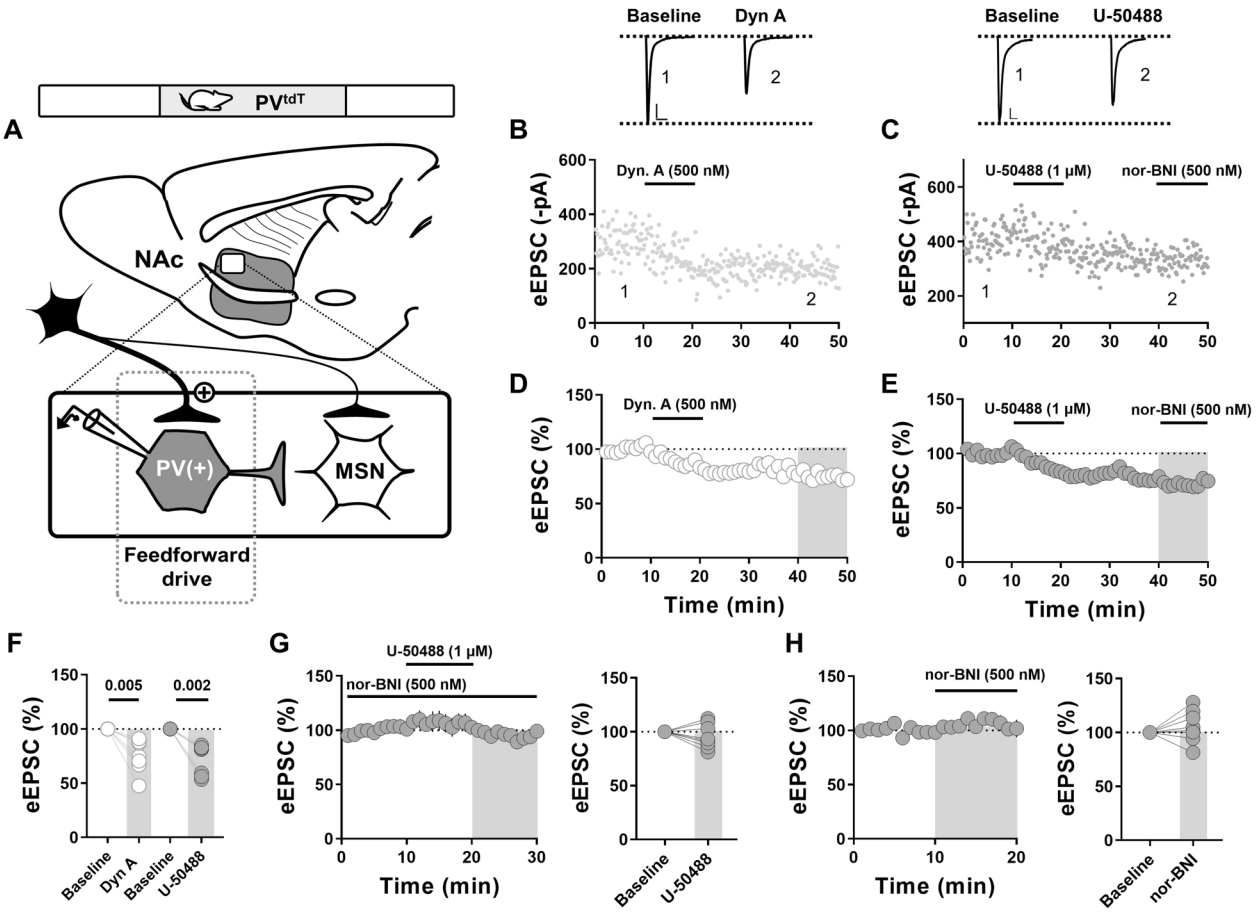

Fig. 1 Kappa opioid receptor stimulation triggers a long-term depression of excitatory transmission onto NAc core PV-FSIs. A Sagittal mouse brain slice representing location of electrophysiological recordings in the dorsomedial NAc core. **B** Representative experiment of eEPSC amplitudes before, during, and post Dynorphin A (500 nM) drug wash from NAc core PV-FSIs, and representative current traces from the first and last ten minutes of the experiment. **C** Representative experiment of eEPSC amplitudes before, during, and post U-50488 (1 μM) drug wash and nor-BNI antagonist (500 nM) chase from NAc core PV-FSIs, and representative current traces from the first and last ten minutes of the experiment. **D** Time-course summary of normalized eEPSCs in PV-FSIs depicting a Dyn. A triggered depression that persists following drug washout. **E** Time-course summary of normalized eEPSCs in PV-FSIs depicting U-50488 triggered long-term depression. **F** Average eEPSC amplitudes taken from baseline and 40–50 min for Dyn. A and U-50488 drug washes (Dyn. A: 75.0 ± 5.8%, n = 7; U-50488: 71.4 ± 5.4%, $n = 7$). **G** Time-course summary of U-50488 (1 μM) washes in the presence of nor-BNI (500 nM) with average eEPSC amplitudes taken from baseline and 20–30 min (95.7 ± 4.0%, $n = 8$, $p = 0.31$). **H** Time-course summary of nor-BNI (500 nM) washes with average eEPSC amplitudes taken from baseline and 10–20 min (105.5 ± 5.2%, n = 8, p = 0.327). Error bars indicate SEM. Baseline = 0–10 min. Scale bars = 50 pA/10 ms. Gray boxes indicate timepoint used to compare to baseline.

NAcc PV-FSIs EPSCs, we replaced GTP with non-hydrolysable GDPβS in the internal solution to inhibit G-protein signaling. In GDPβS loaded cells, U-50488-induced depression was lost and significantly different from control (containing GTP) (Fig. 2D; Ctl: 71.4 ± 5.4%; GDPβS: 102.6 ± 7.8%, $n = 7$ and 5, $p = 0.007$, unpaired t test). Together, these data are consistent with a postsynaptic, G-protein dependent LTD initiated by KORs.

KOR activation initiates the endocytosis of PV-FSI AMPARs

A canonical signaling pathway for opioid receptors is the activation of GIRK channels, which leads to hyperpolarization of the cell and could explain the decrease in PV-FSI eEPSC amplitude mediated by KORs [38]. To test this, we washed on U-50488 in the presence of Ba^{2+} and recorded eEPSCs from NAcc PV-FSIs. U-50488 triggered LTD in the presence of Ba^{2+}, suggesting LTD is not mediated by Ba^{2+} sensitive potassium channels, including GIRKs (Fig. 3A; U-50488 in Ba^{2+}: 75.0 ± 3.5%, $n = 4$, $p = 0.006$, paired t-test). Consistent with blockage of potassium channels, bath-application of Ba^{2+} was accompanied by a decrease in I_h (Fig. 3A inset). Given the established regulatory relationship between dopamine and the KOR in the midbrain dopaminergic system [39, 40], we tested if dopamine was required for KOR-induced LTD by applying U-50488 in the presence of D1- and D2-like dopamine receptor antagonists SCH 23390 and sulpiride, respectively. Inhibiting D1- and D2-like dopamine receptors had no effect on U-50488 triggered LTD of PV-FSI eEPSCs (Fig. 3B; U-50488 in SCH + Sulp: 68.8 ± 9.2%, $n = 4$, $p = 0.043$, paired t test). GPCR signaling can recruit protein kinase A (PKA) via Gβγ. We determined that the mechanism was PKA dependent by the loss of LTD following application of U-50488 when the PKA antagonist H89 (10 μM) was included in the bath solution, implicating the Gβγ signaling arm of KORs (Fig. 3C; U-50488 in H89: 92.6 ± 3.6%, $n = 6$, $p = 0.090$, paired t-test). The loss of LTD in the presence of H89 was also significantly different from control LTD (Ctl: 71.4 ± 5.4%; H89: 92.6 ± 3.6%, $n = 7$ and 6, $p = 0.009$, unpaired t test). We also report that H89 alone has no effect on the eEPSC amplitude of NAcc PV-FSIs (Fig. 3C inset; H89: 98.3 ± 4.9%, $n = 4$, $p = 0.75$, paired t test, final 10 min compared to first 10 min).

To narrow the intracellular signaling mechanisms recruited by KORs to trigger LTD, we determined whether the effect was calcium dependent by incorporating the fast-acting calcium chelator, BAPTA, into the internal solution. Intracellular BAPTA

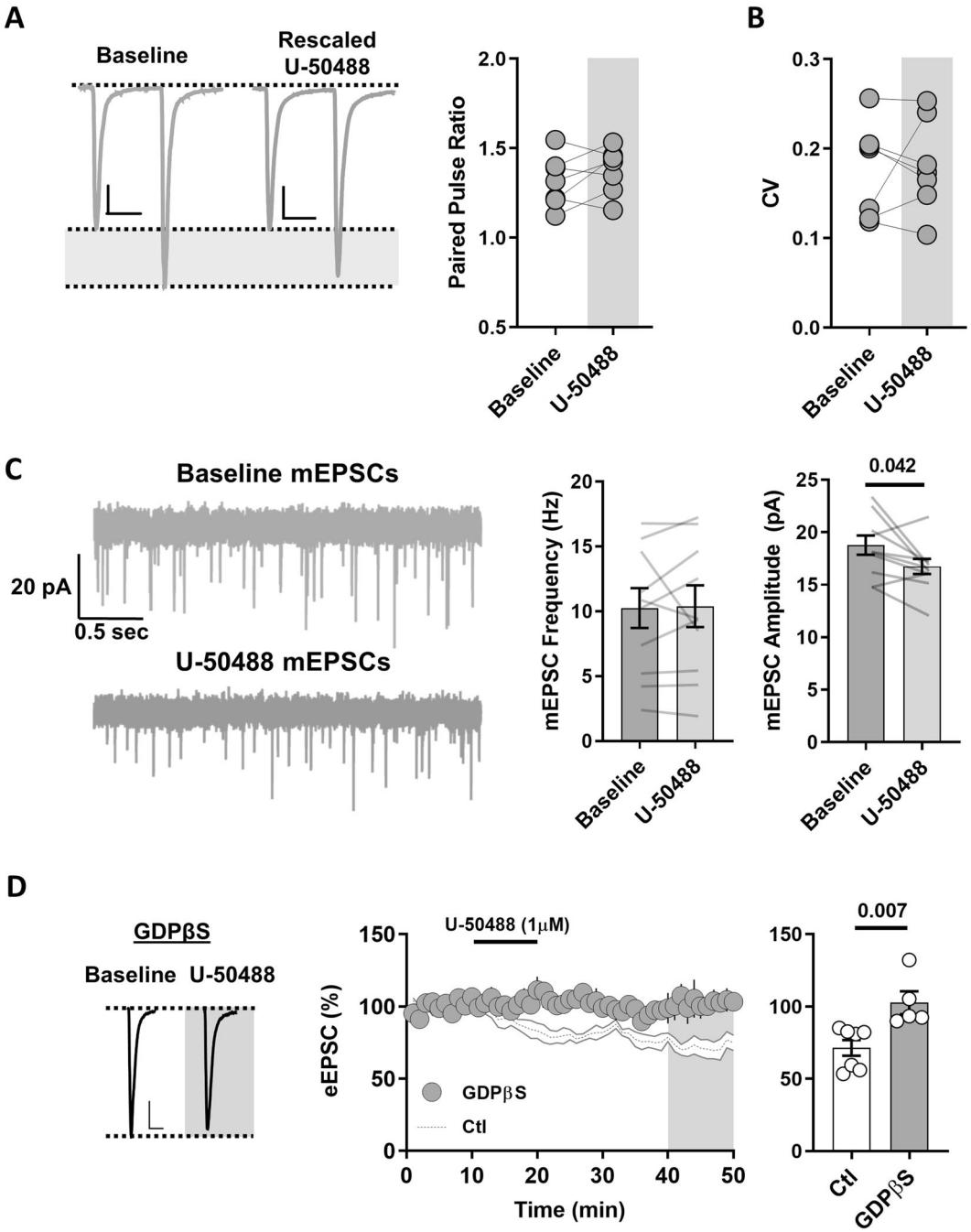

Fig. 2 Kappa opioid receptor mediated long-term depression is expressed post-synaptically. A Representative PPR current traces taken from baseline and 40–50 min (scale bars =50 pA/25 ms). Average PPR taken from baseline and 40–50 min (PPR baseline: 1.32 ± 0.05; PPR 40–50 min: 1.38 ± 0.05, $n = 7$, $p = 0.25$). **B** Average CV taken from baseline and 40–50 min timepoints (CV baseline: 0.18 ± 0.02; CV 40–50 min: 0.18 ± 0.02, $n = 7$, $p = 0.84$). **C** Representative mEPSC traces taken from baseline and 40–45 min timepoints. Average mEPSC frequency taken from 0 to 5 min and 40-45 min timepoints (0–5 min: 10.26 ± 1.53 Hz; 40–45 min: 10.4 ± 1.61 Hz, $n = 10$, $p = 0.87$). Average mEPSC amplitude taken from 0 to 5 min and 40–45 min timepoints (0–5 min: 18.78 ± 0.91 pA; 40–45 min: 16.75 ± 0.72 pA, $n = 10$, $p = 0.042$). **D** Time course summary of U-50488 (1 μM) drug washes in the presence of internally loaded GDPβS or control internal solution, representative current traces from baseline and 40-50 min timepoints for GDPβS loaded cells (scale bars = 50 pA/10 ms), and average eEPSC amplitudes taken from 40 to 50 min for control and GDPβS loaded cells (Ctl: 71.4 ± 5.4%; GDPβS: 102.6 ± 7.8%, $n = 7$ and 5, $p = 0.007$). Gray box represents timepoint used for GDPβS vs Ctl statistics. Error bars indicate SEM. Baseline = 0–10 min.

prevented U-50488-LTD (Fig. 3D; U-50488 with BAPTA: 88.0 ± 10.1%, $n = 6$, $p = 0.290$, paired t test). Given the requirement for calcium in U-50488-LTD of PV-FSI AMPARs, we tested whether the Ca^{2+}/calmodulin-dependent protein phosphatase calcineurin, a downstream effector of Ca^{2+} that has been shown to initiate clathrin-mediated endocytosis of AMPARs [41–44], is responsible for KOR-LTD. We found that incubating slices in calcineurin inhibitor, cyclosporin A, for 1–2 h blocked the ability of U-50488 to trigger LTD (Fig. 3E; U-50488 following cyclosporin A: 103.3 ± 11.3%, $n = 7$, $p = 0.78$, paired t test). The loss of LTD following cyclosporin A incubation was also significantly different from control LTD (Ctl: 71.4 ± 5.4%; cyclosporin A: 103.3 ± 11.3%, $n = 7$

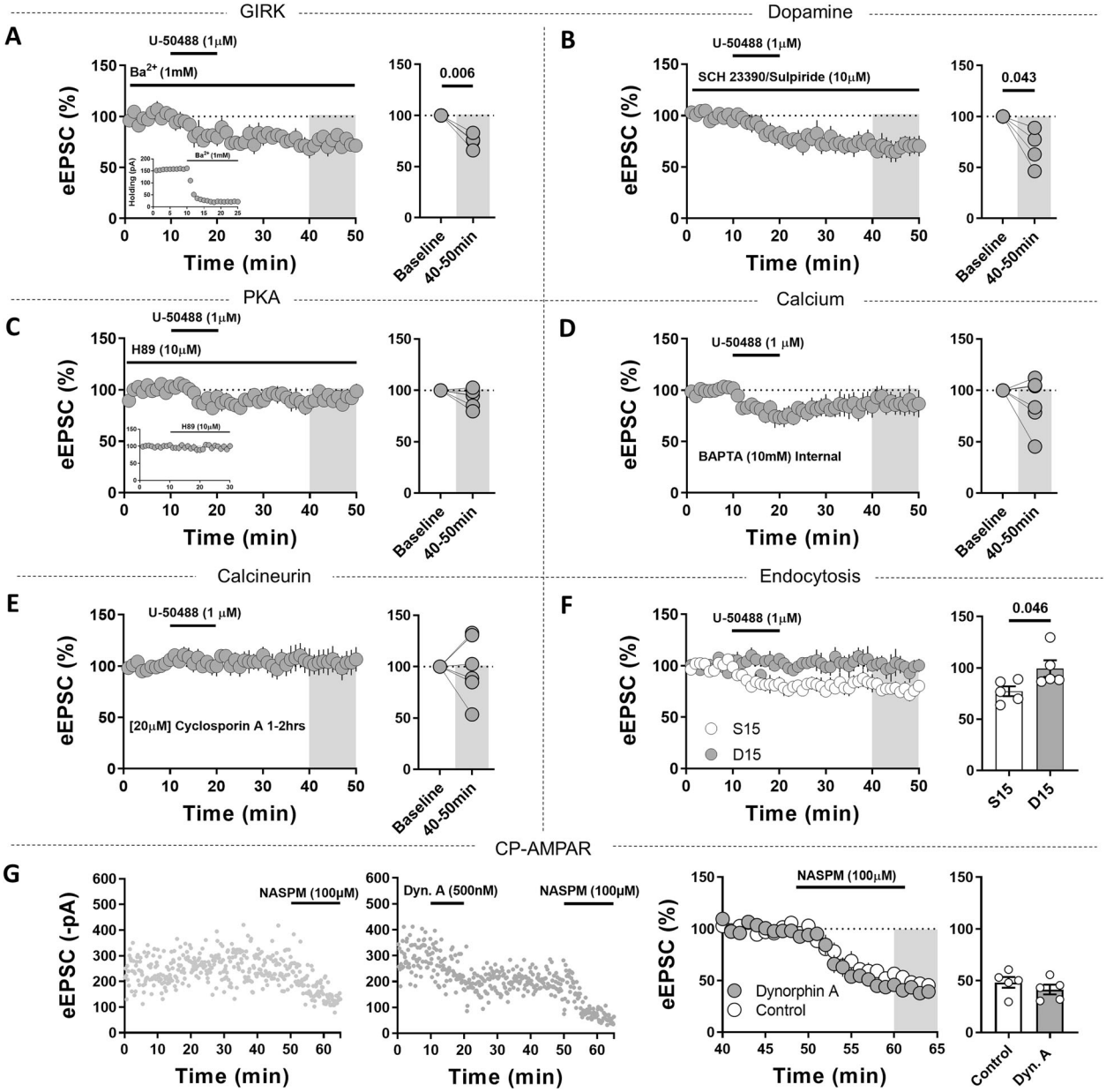

Fig. 3 Kappa opioid receptor activation triggers the endocytosis of PV-FSI AMPARs. A Time-course summary of U-50488 (1 μM) washes in the presence of Ba^{2+}(1 mM) and average eEPSC amplitudes from baseline and 40–50 min (75.0 ± 3.5%, $n = 4$, $p = 0.006$). Inset: representative experiment showing effect of Ba^{2+} on holding current. **B** Time-course summary of U-50488 (1 μM) washes in the presence of SCH 23390/ Sulpiride (10 μM) and average eEPSC amplitudes from baseline and 40–50 min (68.8 ± 9.2%, $n = 4$, $p = 0.043$). **C** Time-course summary of U-50488 (1 μM) washes in the presence of H89 (10 μM) and average eEPSC amplitudes from baseline and 40–50 min (92.6 ± 3.6%, $n = 6$, $p = 0.090$). Inset: time-course summary of the effect of H89 (10 μM) on eEPSC amplitude (98.3 ± 4.9%, $n = 4$, $p = 0.75$, final 10 min compared to first 10 min) (**D**) Time-course summary of U-50488 (1 μM) washes in the presence of cellularly loaded BAPTA (10 mM) and average eEPSC amplitudes from baseline and 40–50 min (88.0 ± 10.1%, $n = 6$, $p = 0.290$). **E** Time-course summary of U-50488 (1 μM) washes in cyclosporin A incubated slices (1–2 h, 20 μM) and average eEPSC amplitudes from baseline and 40–50 min (103.3 ± 11.3%, $n = 7$, $p = 0.78$). **F** Time-course summary of U-50488 (1 μM) washes in cells loaded with either D15 or S15 (2 mM) and average eEPSC amplitudes taken from 40 to 50 min from both groups (S15: 77.2 ± 4.8%; D15: 99.3 ± 8.1%, $n = 5$ and 5, $p = 0.046$). Error bars indicate SEM. Baseline = 0–10 min. Gray boxes indicate timepoint used to compare to baseline in (**A**–**E**), and between S15 and D15 in (**F**). **G** Representative experiments of time-matched control or dynorphin A (500 nM) triggered LTD followed by NASPM (100 μM). Time course summary taken from minutes 40-65 to compare NASPM induced depression between control and dynorphin A (control: 48.4 ± 5.1%; dyn. A: 41.4 ± 4.6, $n = 5$ and 5, $p = 0.34$).

and 7, $p = 0.026$, unpaired t-test). Given this result, we wanted to determine if the activation of KORs was ultimately leading to the trafficking of AMPARs on PV-FSIs. To test this, we introduced the peptide inhibitor D15 (PPPQVPSRPNRAPPG), which blocks the interaction between dynamin and AP1/2 and inhibits the endocytosis of AMPARs, or the scrambled peptide S15 (ANVRRGPPPPPQPSP), into the internal patch solution [45, 46]. U-50488 had no effect on cells loaded with D15, while it elicited a significant depression in cells loaded with S15 compared to those loaded with D15 (Fig. 3F; U-50488 with S15: 77.2 ± 4.8%; D15: 99.3 ± 8.1%, $n = 5$ and 5, $p = 0.046$, unpaired t-test). Previous work from our lab has established that ~50% of EPSC on NAc PV-FSIs is

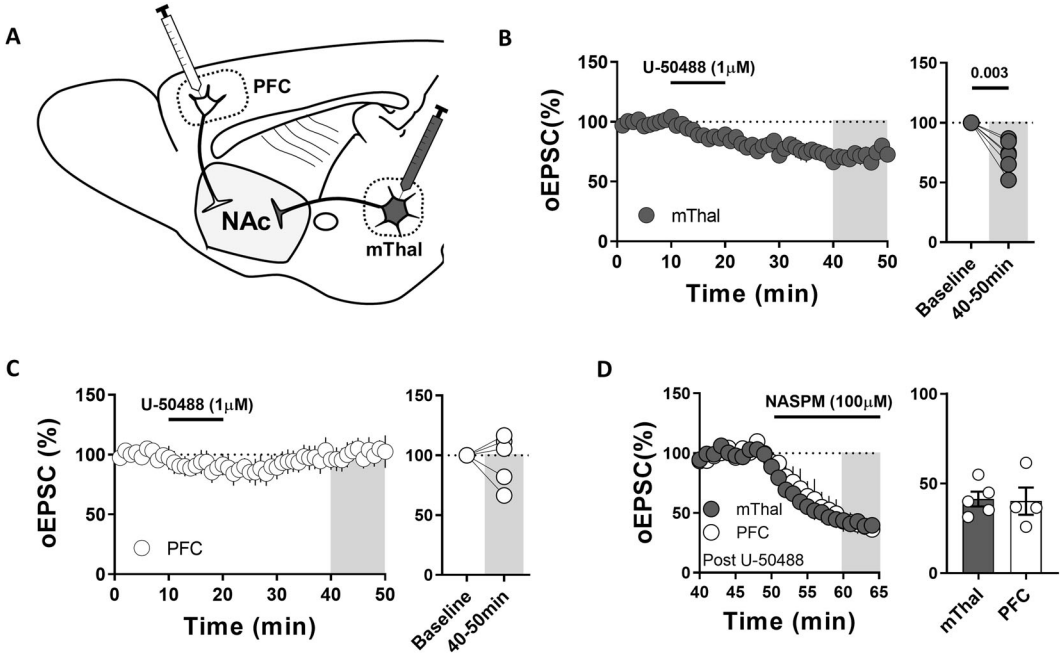

Fig. 4 Kappa opioid receptor preferentially regulates mThal afferents. A Schematic depicting the optogenetic strategy used to isolate PFC or mThal synapses onto NAc core PV-FSIs. **B** Time-course summary of oEPSCs from mThal synapses onto PV-FSIs during U-50488 (1 μM) washes and average oEPSCs from baseline and 40–50 min (72.6 ± 5.3%, $n = 6$, $p = 0.003$). **C** Time-course summary of oEPSCs from PFC synapses onto PV-FSIs during U-50488 (1 μM) washes and average oEPSCs from baseline and 40–50 min (96.4 ± 9.6%, $n = 5$, $p = 0.73$). **D** Time-course summary of oEPSCs from PFC or mThal synapses onto PV-FSIs beginning at the 40 min timepoint following U-50488 (1 μM) wash and through a 15 min wash of NASPM (100 μM) and average oEPSCs from 60 to 65 min compared between the two afferents (PFC: 40.1 ± 7.6%; mThal: 41.3 ± 4.1%, $n = 4$ and 5, $p = 0.89$). Error bars indicate SEM. Baseline = 0–10 min. Gray boxes indicate timepoint used for comparison to baseline in B and C and between mThal and PFC in (**D**).

attributed to calcium permeable AMPARs (CP-AMPARs) with the remainder being resistant to the CP-AMPAR blocker NASPM (calcium impermeable AMPARs, CI-AMPARs) [17]. To determine if KOR-LTD differentially targets the trafficking of CP- or CI-AMPARs we bath applied NASPM following either time-matched control or dynorphin A triggered LTD. We found no difference in NASPM-induced depression of EPSCs, suggesting indiscriminate AMPAR targeting by KORs (Fig. 3G; control: 48.4 ± 5.1%; dyn. A: 41.4 ± 4.6, $n = 5$ and 5, $p = 0.34$, unpaired t test). Taken together, these data suggest that KORs mediate the endocytosis of AMPARs on NAcc PV-FSIs in a PKA/calcineurin-dependent manner.

KOR preferentially regulates mThal afferents

The thalamus is implicated in drug seeking behaviors [47–49], and the thalamic to NAc pathway is required for the expression of opiate withdrawal aversive symptoms [5]. Zhu et al also reports the recruitment of feedforward inhibitory currents in the thalamus to NAc pathway, making this afferent an attractive target for KOR regulation of feedforward inhibitory drive. To test this we injected an adeno-associated virus expressing channelrodopsin2 (AAV-ChR2) into the mThal and recorded optically evoked EPSCs (oEPSCs) in NAcc PV-FSIs (Fig. 4A). U-50488 elicited an LTD of mThal oEPSCs (Fig. 4B; U-50488: 72.6 ± 5.3%, $n = 6$, $p = 0.003$, paired t test). We also note no change in CV following U-50488 application at this synapse (data not shown: CV baseline: 0.16 ± 0.016%; CV 40-50 min: 0.20 ± 0.055%, $n = 6$, $p = 0.33$, paired t test). To determine if KORs on PV-FSIs in the NAcc similarly regulate cortico-accumbens afferents, we injected AAV-ChR2 into the PFC and recorded oEPSCs (Fig. 4A). U-50488 had no effect on oEPSCs from PFC-ChR2 terminals (Fig. 4C; U-50488: 96.4 ± 9.6%, $n = 5$, $p = 0.73$, paired t test). To determine if KOR-LTD of thalamo-accumbens synapses was due to trafficking of CI- or CP-AMPARs, we again washed on NASPM following the 30-min U-50488 washout. There was no difference in depression elicited by NASPM at either the PFC or mThal afferent following U-50488 application (Fig. 4D; PFC: 40.1 ± 7.6%; mThal: 41.3 ± 4.1%, $n = 4$ and 5, $p = 0.89$, unpaired t test), consistent with KOR-LTD of PV-FSIs AMPARs that does not involve the specific targeting of CI- or CP-AMPARs.

KOR-LTD is absent following immobilization stress

Dynorphin is increased in the NAc of persons diagnosed with cocaine use disorder and persons with suicidal ideologies, as well as in rodent models of addiction and depression [25–28]. Immobilization stress has also been shown to increase dynorphin A immunoreactivity in the NAc [50]. To investigate the physiological relevance of KOR- LTD on NAcc PV-FSIs, we used an immobilization paradigm in which mice were restricted in a cylindrical tube for 1 h, allowed to recover for 10 min prior to preparation for electrophysiology assays. U-50488 failed to induce LTD in stressed mice as compared to control mice (Fig. 5A; Stress: 106.8 ± 7.0%; Ctl: 71.4 ± 5.4%, $n = 5$ and 7, $p = 0.002$, unpaired t test). To determine if the loss of U-50488 effect in stressed mice was due to activity at KORs in vivo, 24 h prior to stress mice were given either an IP injection of nor-BNI or saline. Following immobilization stress, U-50488 elicited a significant depression in mice pretreated with nor-BNI compared to saline treated mice (Fig. 5B; Saline: 100.0 ± 4.6%, $n = 7$; nor-BNI: 83.4 ± 2.7%, $n = 6$, $p = 0.012$, unpaired t test). Together, these data suggest that PV-FSI KORs are involved in the response to immobilization stress.

DISCUSSION

Here we describe modulation of feedforward drive onto NAcc PV-FSIs by the dynorphin/KOR system. Using whole-cell patch clamp electrophysiology, pharmacology, and a PV reporter mouse, we find that activating postsynaptic KORs depresses excitatory transmission onto PV-FSIs by triggering the endocytosis of AMPARs via PKA/calcineurin-dependent mechanisms. We provide

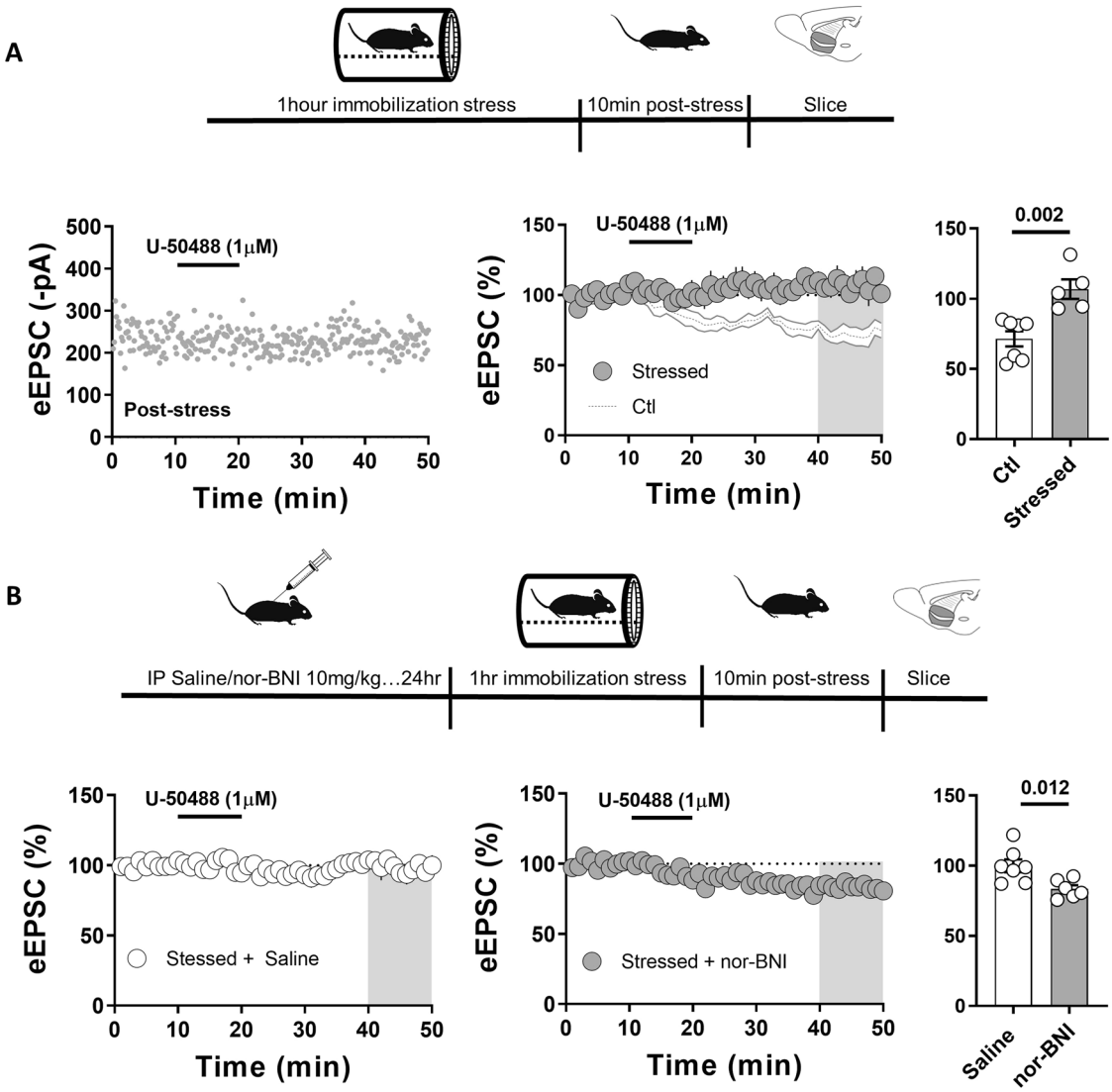

Fig. 5 Kappa opioid receptor agonist does not depress PV-FSI EPSCs following restraint stress and can be rescued by prior administration of the antagonist, nor-BNI. A Above: Schematic depicting immobilization stress paradigm. Below: Representative experiment of eEPSCs collected during U-50488 (1 μM) wash from an immobilization stressed mouse, time course summary of eEPSCs collected during U-50488 (1 μM) washes from immobilization stressed or control (ghosted) mice, and average eEPSC amplitudes from 40 to 50 min compared between stress and control mice (Stress: 106.8 ± 7.0%; Ctl: 71.4 ± 5.4%, $n = 5$ and 7, $p = 0.002$). **B** Above: Schematic depicting nor-BNI or saline administration prior to immobilization stress paradigm. Below: Time-course summaries of eEPSCs collected during U-50488 (1 μM) washes from IP saline or nor-BNI (10 mg/kg) administered mice prior to immobilization stress and average eEPSC amplitudes from 40 to 50 min compared between saline and nor-BNI groups (Saline: 100.0 ± 4.6%, $n = 7$; nor-BNI: 83.4 ± 2.7%, $n = 6$, $p = 0.012$). Error bars indicate SEM. Gray boxes indicate timepoint used for comparison between treatment groups.

evidence for afferent-specific regulation of excitatory drive onto these cells, with mThal but not PFC synapses exhibiting KOR-LTD. Finally, we show that immobilization stress prevents U-50488 depression of glutamatergic transmission that is rescued by prior in vivo administration of the KOR antagonist, nor-BNI. Together, these findings provide evidence for the modulation of NAcc microcircuits via the dynorphin/KOR system, and the involvement of these mechanisms in the response to stress.

The predominant locus of KOR function at excitatory synapses onto MSNs is presynaptic, despite imaging data showing pre- and post-synaptic KOR expression [30, 31, 33, 36]. This manuscript provides the first evidence for postsynaptic KOR mediated regulation of neurotransmission in the NAc. Work from the O'Donnell lab has shown presynaptic inhibition of PFC and hippocampal (HP) inputs onto NAc MSNs in rats [32]. In contrast, Tejeda et al. show that BLA but not HP inputs onto NAc MSNs are inhibited by KORs in mice [33]. Our studies address PFC and mThal afferents into the NAcc of mice and differs from the O'Donnell group in that we see little effect of KOR activation at the PFC input. These studies highlight possible species differences in KOR function as PFC and HP afferents are regulated in rats and BLA and mThal afferents in mice. It is also important to note that the current study is the first to examine KOR regulation of excitatory drive onto PV-FSIs. While PV-FSIs in the NAc receive the same collateralizing afferents as MSNs, it is possible that the collateralizing axons express different molecular regulators. Further characterization of afferent specific regulation by KORs in the NAc across species and cell types will be important for the field.

Prior studies described presynaptic mechanisms by which the KOR inhibits glutamate release onto NAc shell MSNs downstream of Ca^{2+} entry, an effect reversed by nor-BNI [31, 36]. These results differ significantly from the clear postsynaptic and non-reversible

LTD shown here. Differences in these mechanisms may be ascribed to the different cell types being examined, PV-FSIs vs MSNs. Anatomical differences may also play a role as we exclusively recorded from cells in the rostral NAc core while Fields' group recorded in the NAc shell. Behavioral data suggests that KORs along the rostro-caudal axis can differentially regulate hedonic or aversive behaviors, providing behavioral precedent for differing KOR function depending upon the subregion of the NAc [51, 52]. Like the Fields' group we do see a range of depression percentages upon KOR activation. However, in contrast we see a depression in all cells recorded. It is possible that this range of depressions we see is due to a density difference of specific afferent synapses onto PV-FSIs.

The balance between PKA and calcineurin activity is vitally important for both long-term potentiation (LTP) and LTD of excitatory synapses, often both being required for plasticity to occur [53, 54, 55]. KOR activation has been well characterized to lead to PKC_{zeta} and Ca^{2+}mobilization [56]. Both PKC and Ca^{2+}can activate adenylyl cyclase subtypes to promote cAMP production and PKA activation [57]. We hypothesize this may be a mechanism behind KOR activation of PKA. PKA may then be required to phosphorylate an intermediate regulator of calcineurin, or leading to the release of ER stores of $Ca^{2+}$and thus activating calcineurin. A well-documented mechanism of calcineurin-dependent LTD is the dephosphorylation of Ser845 on the GluA1 subunit of AMPARs [58–60]. As NAcc PV-FSIs express CI- and CP-AMPARs, both of which can contain GluA1, this would lead to the endocytosis of both receptors. This is supported by the NASPM experiments where no difference was found in NASPM induced depression following U-50488 at the PFC and mThal synapses, as well as no difference in the depression of eEPSCs using NASPM following dynorphin A (Figs. 3 and 4). In summary, our data support KOR-LTD depends on PKA, calcineurin and endocytosis of AMPARs.

The dorsal paraventricular and paratenial nuclei of the mThal project to the NAc and are implicated in affective states [5, 61]. Therefore these nuclei were targeted as in Joffe et al. [62]. The prelimbic region of the medial PFC has been shown to promote the expression of drug seeking behavior and fear learning, and projects to the NAc core [63, 64]. The mThal, but not PFC, input into the NAc is strengthened following chronic social defeat stress, and stimulating mThal – NAc afferents drives real-time place aversion while stimulating PFC – NAc afferents drives place preference [5, 34, 65]. Given the KOR's role in mediating stress and negative affective states, we wanted to determine if KORs differentially regulate these two afferents. KORs exhibited limited control over PFC inputs but triggered LTD at mThal synapses, adding to previous work from our lab characterizing mThal – NAc specific plasticity mechanisms [62, 66–68]. Given the high level of expression of the KOR within the NAc, it is likely that KOR also regulates other NAc inputs, potentially in a stress-dependent manner. Given the robust loss of KOR-LTD following stress in all cells recorded, we believe it is likely that most inputs onto the NAcc PV-FSIs regulated by the KOR are affected by stress.

The NAc is highly implicated in stress-induced behavioral adaptations [65, 68–73]. Dynorphin levels are upregulated in the NAcc and shell of rodents following immobilization stress, and KOR expression is upregulated in the NAc 2 days following a single bout of immobilization stress [50, 74]. We found that restraint stress prevented U-50488-LTD of NAcc PV-FSI EPSCs and that nor-BNI given before the stress rescues the ability of U-50488 to trigger LTD. Similarly, acute stress has been shown to constitutively activate the KOR at a subset of synapses in the ventral tegmental area [75]. These findings provide strong evidence for the involvement of KORs on NAc PV-FSIs in response to immobilization stress.

CONCLUDING REMARKS

The current hypothesis regarding NAc PV-FSIs functional contribution is that they orchestrate the required neuronal ensembles to support motivated behavioral activity [76]. Inputs into the NAc have been shown to drive feedforward inhibition, and in behavioral states where dynorphin is increased in the NAc, such as stress, this feedforward drive could be biased to ensure the proper neuronal ensembles are recruited to initiate the appropriate behavioral response to the stress. An important future direction is to determine if KOR regulation of this feedforward circuit becomes dysregulated following chronic stress, and if so, what affect does this have on behavior. NAc PV-FSIs have been implicated in impulsivity, where chemogenetic and optogenetic silencing of PV-FSIs leads to loss of impulse control [14]. Loss of impulse control is a hallmark of addiction and is evident in stress-induced relapse. KORs on NAc PV-FSIs represent an excellent candidate for the underlying molecular substrate for stress-induced loss of impulse control. Finally, to our knowledge this is the first description of postsynaptic KOR regulation of neurotransmission in the NAc and greatly advances our understanding of how the KOR regulates NAcc microcircuitry.

FUNDING AND DISCLOSURE

This study was supported by National Institute on Drug Abuse R01 DA040630. The authors have no conflicts of interest to declare.

REFERENCES

1. Joffe ME, Grueter CA, Grueter BA. Biological substrates of addiction. WIREs Cogn Sci. 2014;5:151–71.
2. Grueter BA, Rothwell PE, Malenka RC. Integrating synaptic plasticity and striatal circuit function in addiction. Curr Opin Neurobiol. 2012;22:545–51.
3. Pascoli V, Turiault M, Lüscher C. Reversal of cocaine-evoked synaptic potentiation resets drug-induced adaptive behaviour. Nature. 2012;481:71–75.
4. Pascoli V, Terrier J, Espallergues J, Valjent E, O'Connor EC, Lüscher C. Contrasting forms of cocaine-evoked plasticity control components of relapse. Nature. 2014;509:459–64.
5. Zhu Y, Wienecke CFR, Nachtrab G, Chen X. A thalamic input to the nucleus accumbens mediates opiate dependence. Nature. 2016;530:219–22.
6. Creed MC, Lüscher C. Drug-evoked synaptic plasticity: beyond metaplasticity. Curr Opin Neurobiol. 2013;23:553–8.
7. Turner BD, Kashima DT, Manz KM, Grueter CA, Grueter BA. Synaptic plasticity in the nucleus accumbens: lessons learned from experience. ACS Chem Neurosci 2018;9:2114–26.
8. O'Donnell P, Grace AA. Synaptic interactions among excitatory afferents to nucleus accumbens neurons: hippocampal gating of prefrontal cortical input. J Neurosci 1995;15:3622–39.
9. Wright WJ, Schlüter OM, Dong Y. A feedforward inhibitory circuit mediated by cb1-expressing fast-spiking interneurons in the nucleus accumbens. Neuropsychopharmacology. 2017;42:1146–56.
10. Scudder SL, Baimel C, Macdonald EE, Carter AG. Hippocampal-evoked feedforward inhibition in the nucleus accumbens. J Neurosci 2018;38:9091–104.
11. Manz KM, Coleman BC, Grueter CA, Shields BC, Tadross MR, Grueter BA. Noradrenergic signaling disengages feedforward transmission in the nucleus accumbens shell. J Neurosci. 2021;41:3752–63. https://doi.org/10.1523/JNEUROSCI.2420-20.2021.
12. Trouche S, Koren V, Doig NM, Ellender TJ, El-Gaby M, Lopes-Dos-Santos V, et al. A hippocampus-accumbens tripartite neuronal motif guides appetitive memory in space. Cell. 2019;176:1393–406. e16
13. Yu J, Yan Y, Li KL, Wang Y, Huang YH, Urban NN, et al. Nucleus accumbens feedforward inhibition circuit promotes cocaine self-administration. PNAS. 2017;114:E8750–E8759.
14. Pisansky MT, Lefevre EM, Retzlaff CL, Trieu BH, Leipold DW, Rothwell PE. Nucleus accumbens fast-spiking interneurons constrain impulsive action. Biol Psychiatry. 2019;86:836–47.
15. Wang X, Gallegos DA, Pogorelov VM, O'Hare JK, Calakos N, Wetsel WC, et al. Parvalbumin interneurons of the mouse nucleus accumbens are required for amphetamine-induced locomotor sensitization and conditioned place preference. Neuropsychopharmacology. 2018;43:953–63.

16. Manz KM, Baxley AG, Zurawski Z, Hamm HE, Grueter BA. Heterosynaptic GABAB receptor function within feedforward microcircuits gates glutamatergic transmission in the nucleus accumbens core. J Neurosci 2019;39:9277–93.
17. Manz KM, Ghose D, Turner BD, Taylor A, Becker J, Grueter CA, et al. Calcium-permeable AMPA receptors promote endocannabinoid signaling at parvalbumin interneuron synapses in the nucleus accumbens core. Cell Rep. 2020;32:107971.
18. Tejeda HA, Bonci A. Dynorphin/kappa-opioid receptor control of dopamine dynamics: Implications for negative affective states and psychiatric disorders. Brain Res. 2019;1713:91–101.
19. Van't Veer A, Carlezon WA. Role of kappa-opioid receptors in stress and anxiety-related behavior. Psychopharmacology. 2013;229:435–52.
20. Valenza M, Butelman ER, Kreek MJ. "Effects of the novel relatively short-acting kappa opioid receptor antagonist LY2444296 in behaviors observed after chronic extended-access cocaine self-administration in rats". Psychopharmacology. 2017;234:2219–31.
21. Knoll AT, Carlezon WA. Dynorphin, stress, and depression. Brain Res. 2010;1314:56–73.
22. Bals-Kubik R, Ableitner A, Herz A, Shippenberg TS. Neuroanatomical sites mediating the motivational effects of opioids as mapped by the conditioned place preference paradigm in rats. J Pharm Exp Ther. 1993;264:489–95.
23. Al-Hasani R, McCall JG, Shin G, Gomez AM, Schmitz GP, Bernardi JM, et al. Distinct subpopulations of nucleus accumbens dynorphin neurons drive aversion and reward. Neuron. 2015;87:1063–77.
24. Massaly N, Copits BA, Wilson-Poe AR, Hipólito L, Markovic T, Yoon HJ, et al. Pain-induced negative affect is mediated via recruitment of the nucleus accumbens kappa opioid system. Neuron. 2019;102:564–73. e6
25. Hurd YL, Herkenham M. Molecular alterations in the neostriatum of human cocaine addicts. Synapse. 1993;13:357–69.
26. Hurd YL, Herman MM, Hyde TM, Bigelow LB, Weinberger DR, Kleinman JE. Prodynorphin mRNA expression is increased in the patch vs matrix compartment of the caudate nucleus in suicide subjects. Mol Psychiatry. 1997;2:495–500.
27. Carlezon WA Jr, Thome J, Olson VG, Lane-Ladd SB, Brodkin ES, Hiroi N, et al. Regulation of cocaine reward by CREB. Science. 1998;282:2272–5.
28. Pliakas AM, Carlson RR, Neve RL, Konradi C, Nestler EJ, Carlezon WA Jr. Altered responsiveness to cocaine and increased immobility in the forced swim test associated with elevated camp response element-binding protein expression in nucleus accumbens. J Neurosci 2001;21:7397–403.
29. Svingos AL, Colago EEO, Pickel VM. Cellular sites for dynorphin activation of κ-opioid receptors in the rat nucleus accumbens shell. J Neurosci 1999;19:1804–13.
30. Svingos AL, Chavkin C, Colago EEO, Pickel VM. Major coexpression of κ-opioid receptors and the dopamine transporter in nucleus accumbens axonal profiles. Synapse. 2001;42:185–92.
31. Hjelmstad GO, Fields HL. Kappa opioid receptor activation in the nucleus accumbens inhibits glutamate and gaba release through different mechanisms. J Neurophysiol. 2003;89:2389–95.
32. Brooks JM, O'Donnell P. Kappa opioid receptors mediate heterosynaptic suppression of hippocampal inputs in the rat ventral striatum. J Neurosci 2017;37:7140–8.
33. Tejeda HA, Wu J, Kornspun AR, Pignatelli M, Kashtelyan V, Krashes MJ, et al. Pathway- and cell-specific kappa-opioid receptor modulation of excitation-inhibition balance differentially gates D1 and D2 accumbens. Neuron Act Neuron. 2017;93:147–63.
34. Britt JP, Benaliouad F, McDevitt RA, Stuber GD, Wise RA, Bonci A. Synaptic and behavioral profile of multiple glutamatergic inputs to the nucleus accumbens. Neuron. 2012;76:790–803.
35. Manz KM, Siemann JK, McMahon DG, Grueter BA. Patch-clamp and multi-electrode array electrophysiological analysis in acute mouse brain slices. STAR Protoc. 2021;2:100442.
36. Hjelmstad GO, Fields HL. Kappa opioid receptor inhibition of glutamatergic transmission in the nucleus accumbens shell. J Neurophysiol. 2001;85:1153–8.
37. Mu P, Neumann PA, Panksepp J, Schlüter OM, Dong Y. Exposure to cocaine alters dynorphin-mediated regulation of excitatory synaptic transmission in nucleus accumbens neurons. Biol Psychiatry. 2011;69:228–35.
38. Al-Hasani R, Bruchas MR. Molecular mechanisms of opioid receptor-dependent signaling and behavior. Anesthesiology. 2011;115:1363–81.
39. Margolis EB, Hjelmstad GO, Bonci A, Fields HL. κ-Opioid agonists directly inhibit midbrain dopaminergic neurons. J Neurosci 2003;23:9981–6.
40. Bruchas MR, Land BB, Chavkin C. The dynorphin/kappa opioid system as a modulator of stress-induced and pro-addictive behaviors. Brain Res. 2010;1314:44–55.
41. Unoki T, Matsuda S, Kakegawa W, Van NT, Kohda K, Suzuki A, et al. NMDA receptor-mediated PIP5K activation to produce PI(4,5)P2 is essential for AMPA receptor endocytosis during LTD. Neuron. 2012;73:135–48.
42. Mulkey RM, Endo S, Shenolikar S, Malenka RC. Involvement of a calcineurin/inhibitor-1 phosphatase cascade in hippocampal long-term depression. Nature. 1994;369:486–8.
43. Matsuda S, Kakegawa W, Budisantoso T, Nomura T, Kohda K, Yuzaki M. Stargazin regulates AMPA receptor trafficking through adaptor protein complexes during long-term depression. Nat Commun. 2013;4:2759.
44. Chávez AE, Chiu CQ, Castillo PE. TRPV1 activation by endogenous anandamide triggers postsynaptic long-term depression in dentate gyrus. Nat Neurosci. 2010;13:1511–8.
45. Grueter BA, Brasnjo G, Malenka RC. Postsynaptic TRPV1 triggers cell type–specific long-term depression in the nucleus accumbens. Nat Neurosci. 2010;13:1519–25.
46. Lüscher C, Xia H, Beattie EC, Carroll RC, von Zastrow M, Malenka RC, et al. Role of AMPA receptor cycling in synaptic transmission and plasticity. Neuron. 1999;24:649–58.
47. Browning JR, Jansen HT, Sorg BA. Inactivation of the paraventricular thalamus abolishes the expression of cocaine conditioned place preference in rats. Drug Alcohol Depend. 2014;134:387–90.
48. Neumann PA, Wang Y, Yan Y, Wang Y, Ishikawa M, Cui R, et al. Cocaine-induced synaptic alterations in thalamus to nucleus accumbens projection. Neuropsychopharmacology. 2016;41:2399–410.
49. James MH, Charnley JL, Jones E, Levi EM, Yeoh JW, Flynn JR, et al. Cocaine- and amphetamine-regulated transcript (CART) signaling within the paraventricular thalamus modulates cocaine-seeking behaviour. PLOS ONE. 2010;5:e12980.
50. Shirayama Y, Ishida H, Iwata M, Hazama GI, Kawahara R, Duman RS. Stress increases dynorphin immunoreactivity in limbic brain regions and dynorphin antagonism produces antidepressant-like effects. J Neurochem. 2004;90:1258–68.
51. Castro DC, Berridge KC. Opioid hedonic hotspot in nucleus accumbens shell: mu, delta, and kappa maps for enhancement of sweetness "liking" and "wanting". J Neurosci 2014;34:4239–50.
52. Pirino BE, Spodnick MB, Gargiulo AT, Curtis GR, Barson JR, Karkhanis AN. Kappa-opioid receptor-dependent changes in dopamine and anxiety-like or approach-avoidance behavior occur differentially across the nucleus accumbens shell rostro-caudal axis. Neuropharmacology. 2020;181:108341.
53. Esteban JA, Shi SH, Wilson C, Nuriya M, Huganir RL, Malinow R. PKA phosphorylation of AMPA receptor subunits controls synaptic trafficking underlying plasticity. Nat Neurosci. 2003;6:136–43.
54. Beattie EC, Carroll RC, Yu X, Morishita W, Yasuda H, von Zastrow M, et al. Regulation of AMPA receptor endocytosis by a signaling mechanism shared with LTD. Nat Neurosci. 2000;3:1291–1300.
55. Sanderson JL, Gorski JA, Dell'Acqua ML. NMDA receptor-dependent LTD requires transient synaptic incorporation of Ca2+-permeable AMPARs mediated by AKAP150-anchored PKA and calcineurin. Neuron. 2016;89:1000–15.
56. Belcheva MM, Clark AL, Haas PD, Serna JS, Hahn JW, Kiss A, et al. μ and κ Opioid Receptors Activate ERK/MAPK via Different Protein Kinase C Isoforms and Secondary Messengers in Astrocytes*. J Biol Chem. 2005;280:27662–9.
57. Halls ML, Cooper DMF. Regulation by Ca2+-signaling pathways of adenylyl cyclases. Cold Spring Harb Perspect Biol. 2011;3:a004143.
58. Mulkey RM, Herron CE, Malenka RC. An essential role for protein phosphatases in hippocampal long-term depression. Science. 1993;261:1051–5.
59. Kam AYF, Liao D, Loh HH, Law P-Y. Morphine induces AMPA receptor internalization in primary hippocampal neurons via calcineurin-dependent dephosphorylation of GluR1 subunits. J Neurosci 2010;30:15304–16.
60. Derkach VA, Oh MC, Guire ES, Soderling TR. Regulatory mechanisms of AMPA receptors in synaptic plasticity. Nat Rev Neurosci. 2007;8:101–13.
61. Vertes RP, Linley SB, Hoover WB. Limbic circuitry of the midline thalamus. Neurosci Biobehav Rev. 2015;54:89–107.
62. Joffe ME, Grueter BA. Cocaine experience enhances thalamo-accumbens N-methyl-D-aspartate receptor function. Biol Psychiatry. 2016;80:671–81.
63. Pietro NCD, Black YD, Kantak KM. Context-dependent prefrontal cortex regulation of cocaine self-administration and reinstatement behaviors in rats. Eur J Neurosci. 2006;24:3285–98.
64. Corcoran KA, Quirk GJ. Activity in prelimbic cortex is necessary for the expression of learned, but not innate, fears. J Neurosci. 2007;27:840–4.
65. Christoffel DJ, Golden SA, Walsh JJ, Guise KG, Heshmati M, Friedman AK, et al. Excitatory transmission at thalamo-striatal synapses mediates susceptibility to social stress. Nat Neurosci. 2015;18:962–4.
66. Joffe ME, Turner BD, Delpire E, Grueter BA. Genetic loss of GluN2B in D1-expressing cell types enhances long-term cocaine reward and potentiation of thalamo-accumbens synapses. Neuropsychopharmacology. 2018;43:2383–9.
67. Turner BD, Rook JM, Lindsley CW, Conn PJ, Grueter BA. mGlu1 and mGlu5 modulate distinct excitatory inputs to the nucleus accumbens shell. Neuropsychopharmacology. 2018;43:2075–82.
68. Manz KM, Becker JC, Grueter CA, Grueter BA. Histamine H3 receptor function biases excitatory gain in the nucleus accumbens. Biol Psychiatry. 2021;89:588–99.

69. LaPlant Q, Vialou V, Covington HE, Dumitriu D, Feng J, Warren BL, et al. Dnmt3a regulates emotional behavior and spine plasticity in the nucleus accumbens. Nat Neurosci. 2010;13:1137–43.
70. Krishnan V, Han MH, Graham DL, Berton O, Renthal W, Russo SJ, et al. Molecular adaptations underlying susceptibility and resistance to social defeat in brain reward regions. Cell. 2007;131:391–404.
71. Heshmati M, Christoffel DJ, LeClair K, Cathomas F, Golden SA, Aleyasin H, et al. Depression and social defeat stress are associated with inhibitory synaptic changes in the nucleus accumbens. J Neurosci 2020;40:6228–33.
72. Francis TC, Chandra R, Friend DM, Finkel E, Dayrit G, Miranda J, et al. Nucleus accumbens medium spiny neuron subtypes mediate depression-related outcomes to social defeat stress. Biol Psychiatry. 2015;77:212–22.
73. Lim BK, Huang KW, Grueter BA, Rothwell PE, Malenka RC. Anhedonia requires MC4R-mediated synaptic adaptations in nucleus accumbens. Nature. 2012;487:183–9.
74. Lucas LR, Dragisic T, Duwaerts CC, Swiatkowski M, Suzuki H. Effects of recovery from immobilization stress on striatal preprodynorphin- and kappa opioid receptor-mRNA levels of the male rat. Physiol Behav. 2011;104:972–80.
75. Polter AM, Barcomb K, Chen RW, Dingess PM, Graziane NM, Brown TE, et al. Constitutive activation of kappa opioid receptors at ventral tegmental area inhibitory synapses following acute stress. eLife. 2017;6:e23785.
76. Schall TA, Wright WJ, Dong Y. Nucleus accumbens fast-spiking interneurons in motivational and addictive behaviors. Mol Psychiatry. 2021;26:234–46.

AUTHOR CONTRIBUTIONS

BCC, KMM, and BAG designed experiments. Animal breeding, behavioral testing, data analysis, and the construction of the manuscript was performed by BCC, KMM, and BAG. BCC and KMM performed experiments. All authors contributed to editing and revisions of the manuscript.

ADDITIONAL INFORMATION

Correspondence and requests for materials should be addressed to B.A.G.